

## Supporting Information

### Allosteric communication disrupted by small molecule binding to the Imidazole glycerol phosphate synthase protein-protein interface.

*Ivan Rivalta<sup>\*,§,#</sup>, George P. Lisi<sup>#</sup>, Ning-Shiuan Snoeberger<sup>#</sup>, Gregory Manley<sup>#</sup>, J. Patrick Loria<sup>\*,#,‡</sup> and Victor S. Batista<sup>\*,#</sup>*

<sup>§</sup>Univ Lyon, Ens de Lyon, CNRS, Université Lyon 1, Laboratoire de Chimie UMR 5182, F-69342, Lyon, France. <sup>#</sup>Department of Chemistry and <sup>‡</sup>Department of Molecular Biophysics and Biochemistry Yale University, P.O. Box 208107, New Haven, CT 06520-8107, USA.

### Table of content

- **Figure S1.** Hydrophobic contacts at the bottom of the HisF barrel in the apo, PRFAR-bound binary and ternary complexes.
- **Table S1.** Average distances of hydrophobic contacts at the effector site.
- **Figure S2.** Relative positions of the  $\alpha 2$  and  $\alpha 3$  helices in the apo, PRFAR-bound binary and ternary complexes.
- **Figure S3.** The influence of the inhibitor binding on the ammonia gate.
- **Figure S4.** Chemical shift perturbations in the HisF domain of apo PRFAR-bound IGPS upon titration with 3.
- **Figure S5.** Representative correlation peaks from  $^1\text{H}$ - $^{15}\text{N}$  HSQC NMR experiments of  $^{15}\text{N}$ -labeled HisF-IGPS.
- **Figure S6.** Chemical shifts changes in apo IGPS induced by binding of 3.
- **Table S2.**  $^{15}\text{N}$  Chemical shift perturbations of HisH residues upon titration of apo IGPS with 3
- **Figure S7.** Representative correlation peaks from  $^1\text{H}$ - $^{15}\text{N}$  HSQC NMR experiments of  $^{15}\text{N}$ -labeled HisF-IGPS.
- **Figure S8.** Chemical shifts changes in PRFAR-bound IGPS induced by binding of 3.
- **Figure S9.** Breathing motion of the PRFAR-bound 3-IGPS ternary complexes.
- **References**

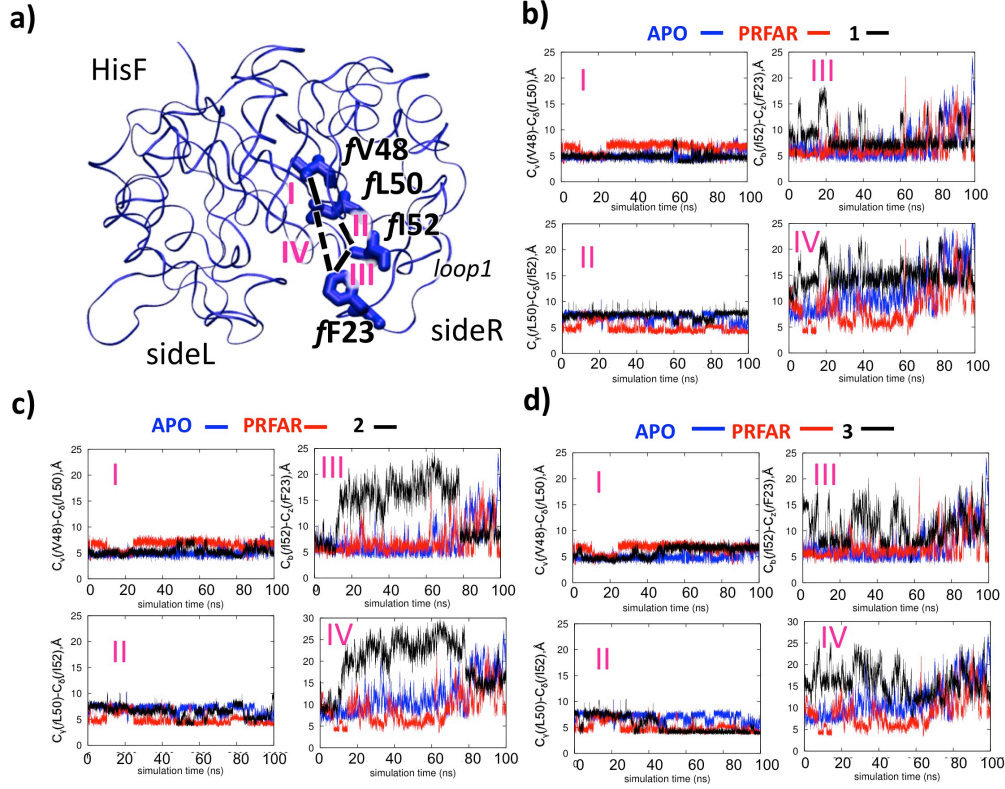


**Figure S1. Hydrophobic contacts at the bottom of the HisF barrel in the apo, PRFAR-bound binary and ternary complexes.** The distances (in Å) between amino acid residues with hydrophobic side chains, i.e. fV48, fL50 and fI52 (a), are monitored along the 0.1  $\mu$ s MD simulations of the apo (blue), binary PRFAR-bound (red) and the ternary complexes (in black) with potential inhibitors 1-3 (b-d).

**Table S1. Average distances (in Å) between hydrophobic amino acid residues at the bottom of the HisF barrel in the apo, PRFAR-bound binary and ternary complexes.** The hydrophobic contacts defining the measured distances (with Roman numerals) are defined in Figure S1.

	apo	PRFAR	1	2	3
(I) fV48-fL50	5.02	6.58	4.84	5.24	5.86
(II) fL50-fI52	6.97	5.02	7.40	6.47	5.45
(III) fI52-fF23	7.23	6.98	8.54	13.85	10.57
(IV) fL50-fF23	11.77	8.91	14.99	19.97	15.86
(II)+(III)+(IV)	25.79	20.91	30.93	40.29	31.88

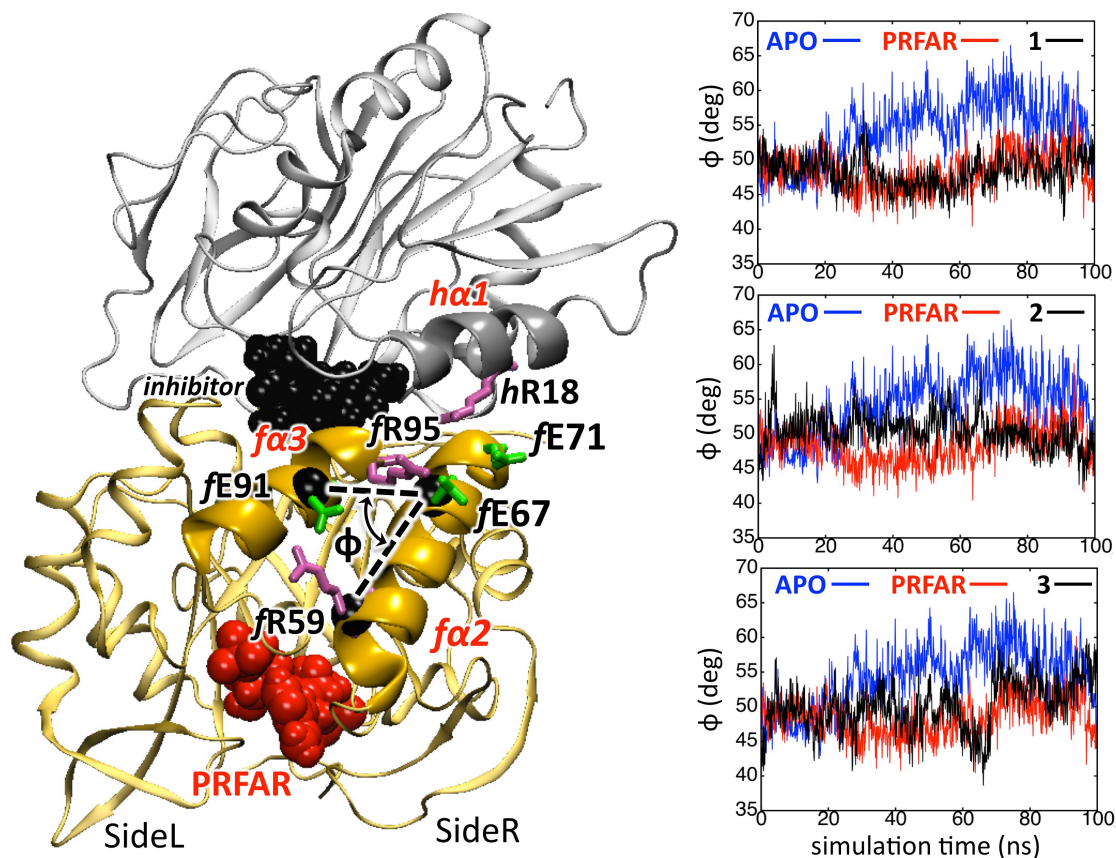


**Figure S2. Relative positions of the *fa2* and *fa3* helices in the apo, PRFAR-bound binary and ternary complexes.** The charged amino acid residues in the *fa2* and *fa3* helices are involved in specific contacts (left panel) that induce different relative positions of the two helices in the apo and PRFAR-bound complexes, taking an active part in the IGPS allosteric mechanism. The relative positions of the two helices are monitored (right panels) in along the 0.1  $\mu$ s MD simulations of the apo (blue), binary PRFAR-bound (red) and the ternary complexes (in black) with potential inhibitors **1-3**.

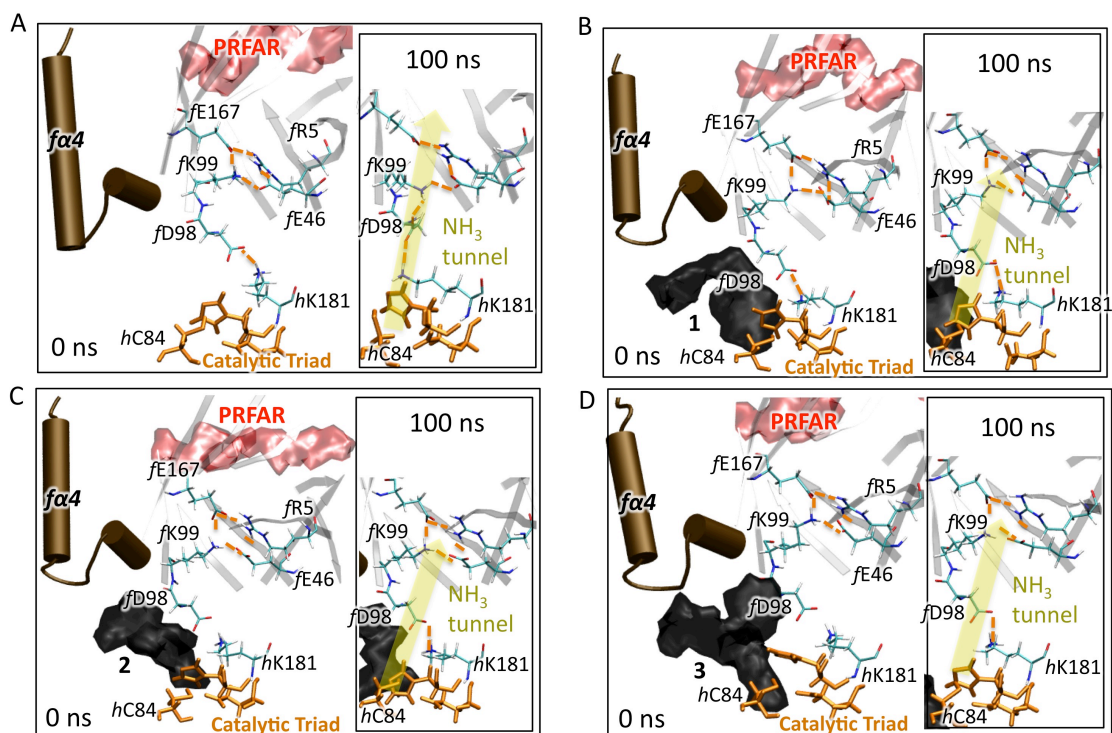


**Figure S3. The influence of the inhibitor binding on the ammonia gate.** Residues *f*R5, *f*E46, *f*K99, and *f*E167 create salt bridges that serve as ammonia gate for the HisF ( $\beta/\alpha$ )<sub>8</sub> barrel that opens within 100 ns in the MD trajectory of the PRFAR-bound binary complex (A), as expected for an active IGPS conformation, due to interactions between *f*K99 and *f*D98 side chains. When the inhibitors **1-3** bind (B-D) the gate remain closed due to the altered dynamics of *f*D98 induced by the interfacial ligands.

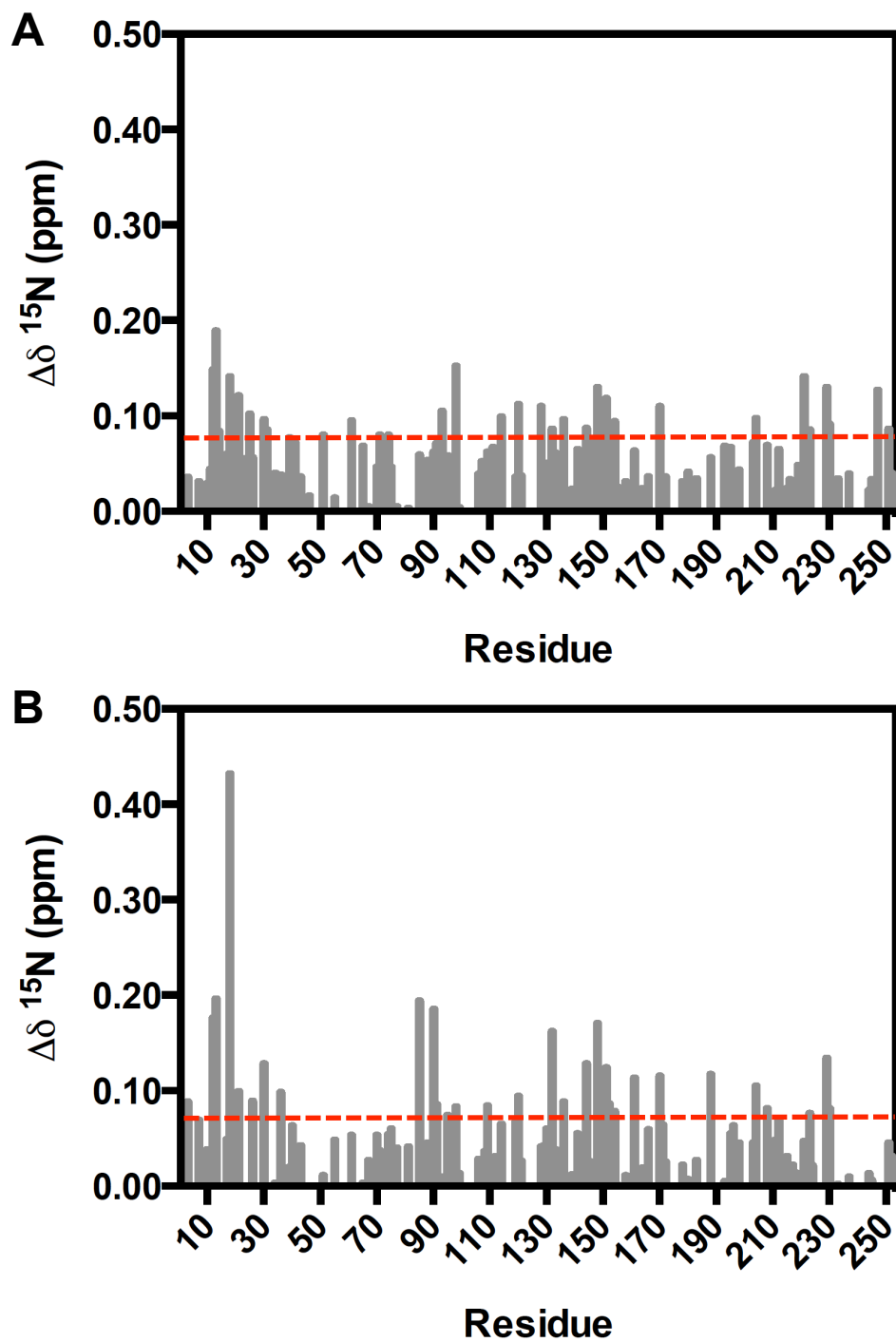


**Figure S4. Chemical shift perturbations in the HisF domain of (A) apo IGPS and (B) PRFAR-bound IGPS upon titration with 3.** The red line represents the 10% trimmed mean of all shifts, and perturbations greater than this cutoff are deemed significant.

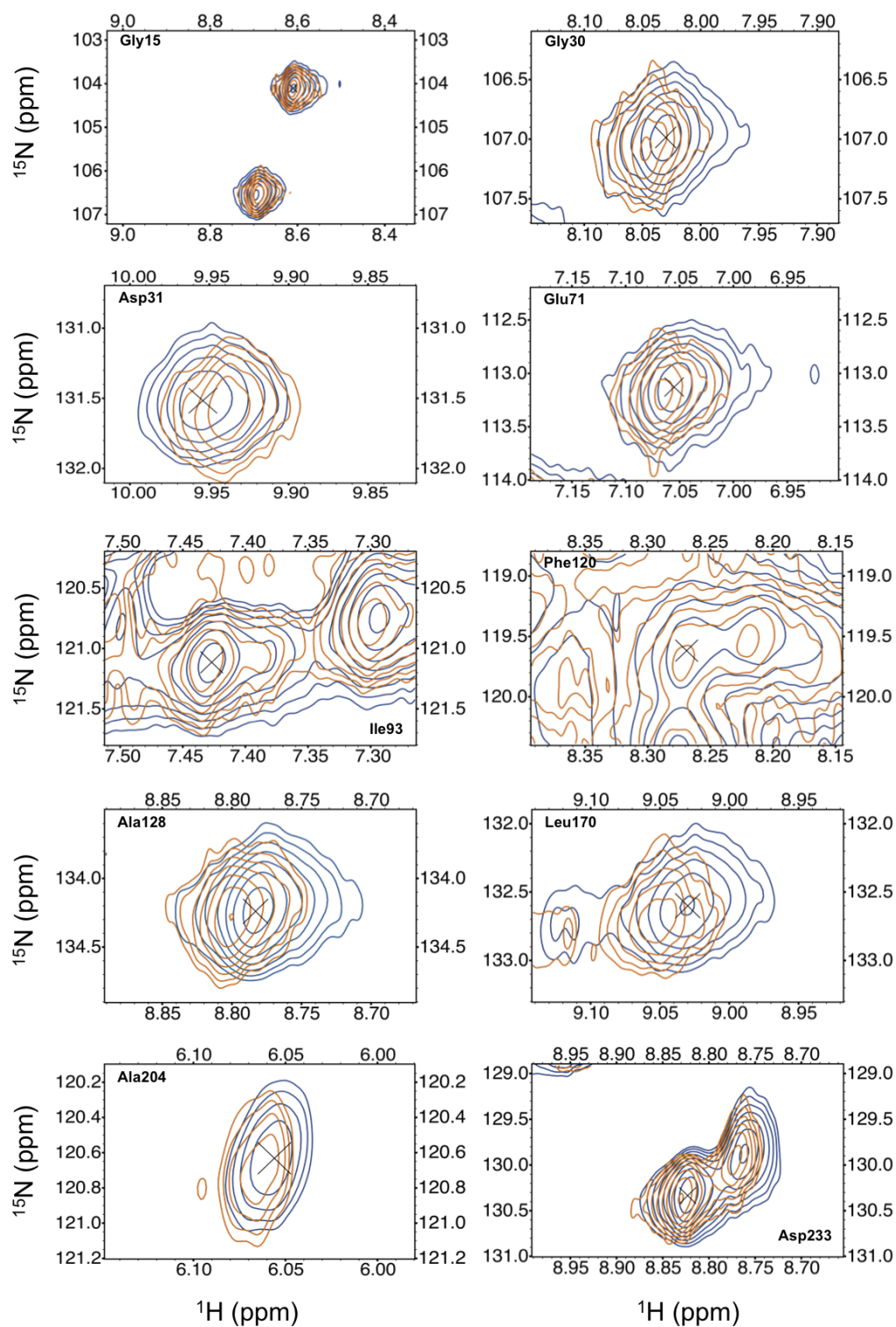


**Figure S5. Representative correlation peaks from  $^1\text{H}$ - $^{15}\text{N}$  HSQC NMR experiments of  $^{15}\text{N}$ -labeled HisF-IGPS.** Titration of **3** into apo IGPS (blue) to a concentration of 3.17 mM (orange) causes distinct shifts in several resonances (Gly30, Asp31, Glu71, etc), while others remain unchanged (Gly15, Ile93). Significant chemical shift differences ( $\Delta\delta$ ) are summarized in Figure S6.



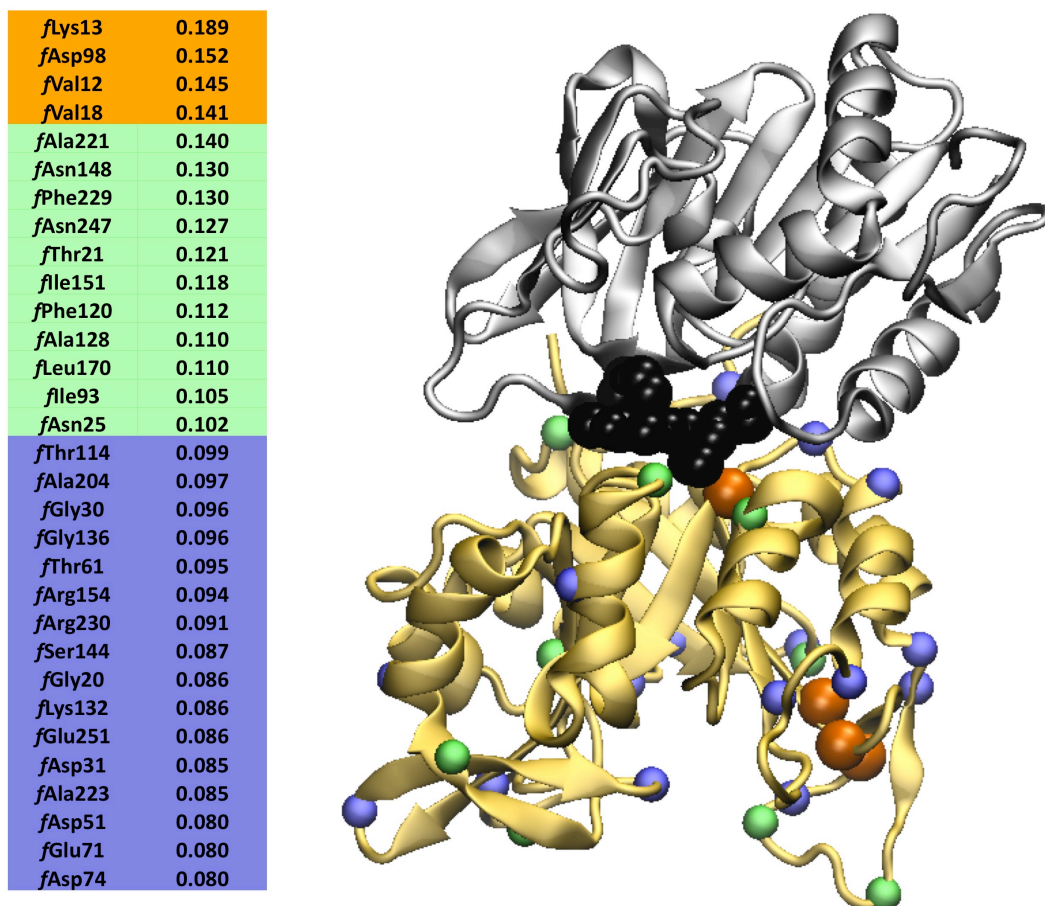


**Figure S6. Chemical shifts changes in apo IGPS induced by binding of 3.** Titration of **3** into apo IGPS (blue) to a concentration of 3.17 mM (orange) causes distinct shifts in several resonances (listed in the left panel). Residues with  $\Delta\delta > 0.14$  (orange balls at C $\alpha$ ),  $\Delta\delta > 0.10$  (light green) and  $\Delta\delta > 0.08$  (blue balls) are mapped onto the **3**-IGPS structure. Chemical shifts are determined by  $^1\text{H}$ - $^{15}\text{N}$  HSQC NMR experiments of  $^{15}\text{N}$ -labeled HisF-IGPS.

**Table S2.  $^{15}\text{N}$  Chemical shift perturbations of HisH residues upon titration of apo IGPS with 3 (3.2 mM). Residues with  $\Delta\delta > 0.06$  ppm were determined to be statistically significant from the 10% trimmed mean.**

<i>Residue</i>	$\Delta\delta$ (ppm)
<i>Arg18</i>	0.092
<i>Ser24</i>	0.077
<i>Ile32</i>	0.200
<i>Phe54</i>	0.051
<i>Gly55</i>	0.076
<i>Leu66</i>	0.061
<i>Phe69</i>	0.071
<i>Glu92</i>	0.140
<i>Glu95</i>	0.061
<i>Thr155</i>	0.065
<i>Arg200</i>	0.076



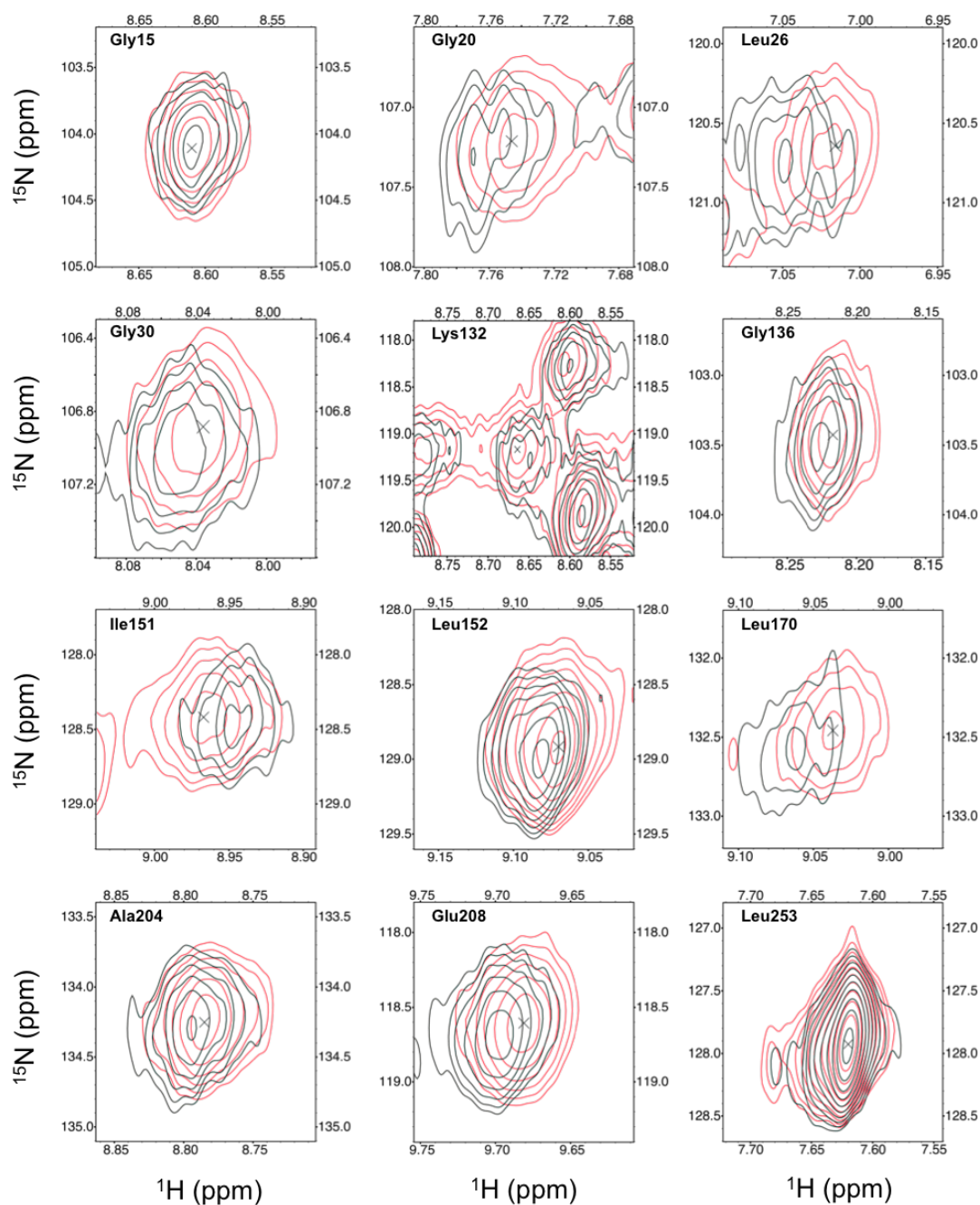


**Figure S7. Representative correlation peaks from  $^1\text{H}$ - $^{15}\text{N}$  HSQC NMR experiments of  $^{15}\text{N}$ -labeled HisF-IGPS.** Titration of PRFAR into apo IGPS to a concentration of 0.96 mM (red) causes distinct shifts in several resonances, and titration of **3** into the binary complex to a concentration of 9.2 mM (black) causes further perturbation. Significant chemical shift differences ( $\Delta\delta$ ) are summarized in Figure S8.

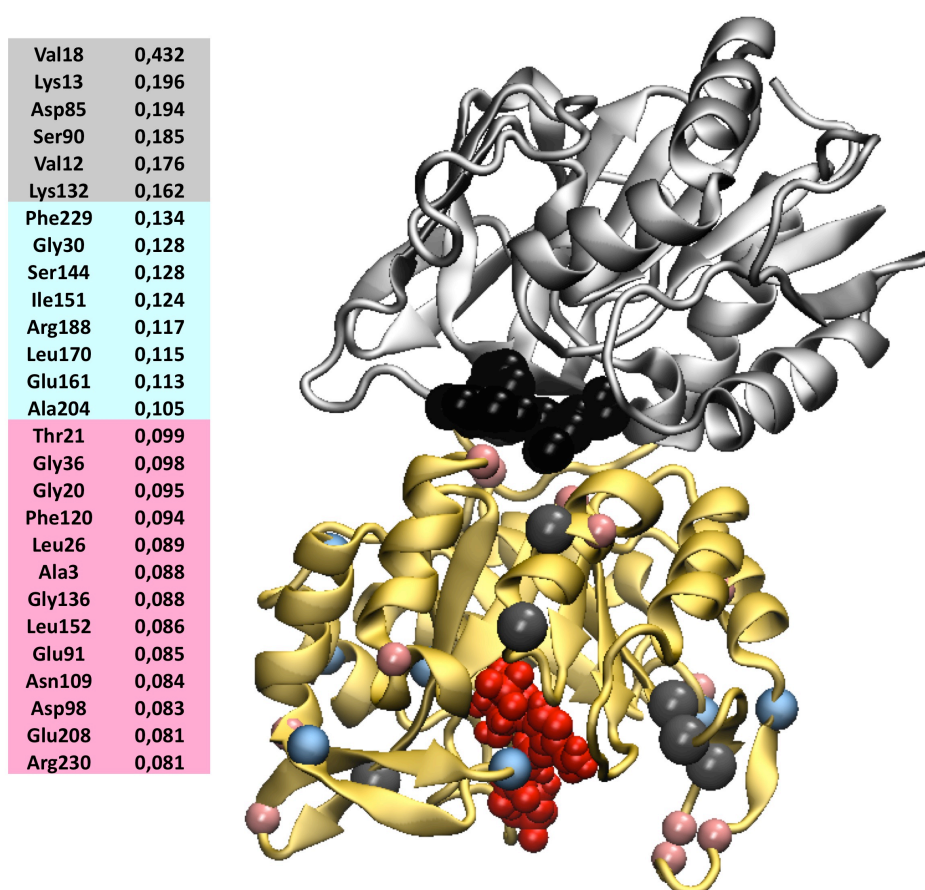


**Figure S8. Chemical shifts changes in PRFAR-bound IGPS induced by binding of 3.** Titration of **3** into binary IGPS (red) to a concentration of 9.2 mM (grey) causes distinct shifts in several resonances (listed in the left panel). Residues with  $\Delta\delta > 0.14$  (grey balls),  $\Delta\delta > 0.10$  (light blue) and  $\Delta\delta > 0.08$  (pink balls) are mapped onto the 3-IGPS structure. Chemical shifts are determined by  $^1\text{H}$ - $^{15}\text{N}$  HSQC NMR experiments of  $^{15}\text{N}$ -labeled HisF of the binary IGPS complex, with PRFAR concentration of 0.96 mM.

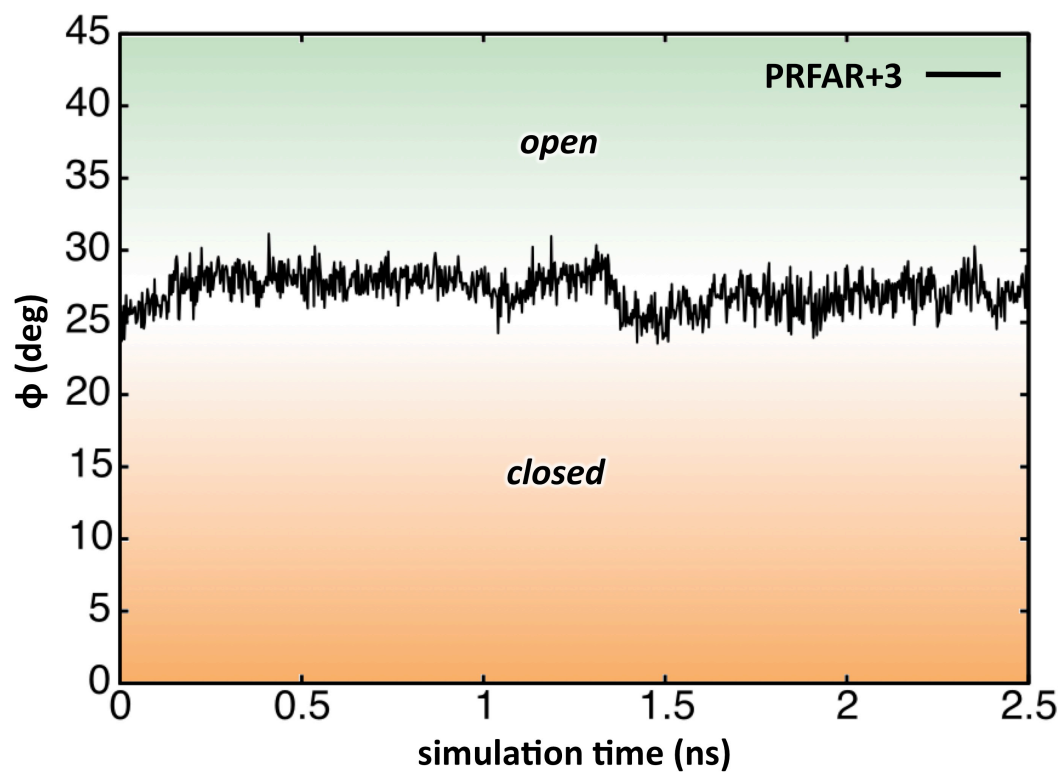


**Figure S9. Breathing motion of the PRFAR-bound 3-IGPS ternary complexes.** The breathing motion is measured by the angle ( $\phi$ ) defined by the C $\alpha$  of the *f*F120, *h*W123 and *h*G52 (see main text). The evolution of  $\phi$  during the MD simulation time (0-2.5  $\mu$ s) is reported.